# Synchronized biphotonic process triggering C−C coupling catalytic reactions

Carmen G. López-Calixto, Marta Liras, Victor A. de la Peña O'Shea*, Raúl Pérez-Ruiz*

*Photoactivated Processes Unit, IMDEA Energy, Av. Ramón de la Sagra 3, Parque Tecnológico de Móstoles, 28935, Móstoles, Madrid, Spain*

## ARTICLE INFO

## ABSTRACT

Activation of aryl(Ar)-halides for C−C coupling catalytic reactions using visible light has become one of the most challenging tasks in organic synthesis since it offers effective and safer alternatives to traditional dehalogenation protocols. The insufficient energy provided by visible light to cleave such strong C−H alogen bonds certainly makes necessary the development of new protocols to overcome this limitation. We report here the application of photon upconversion (UC) technology based on triplet-triplet annihilation (TTA) to a C−C coupling catalytic reaction, a possibility that has not been investigated to date. This synchronized biphotonic process (TTA-UC) activates successfully Ar-halides with visible light. Based on product analysis and spectroscopic experiments, a cascade process combining photophysical and photochemical steps is proposed for the mechanism rationalization. Visible light, ambient temperature and pressure, low-loading metal-free photocatalysts and no additives make this protocol very attractive for applications to the synthesis of fine chemical building blocks, pharmaceuticals, agrochemicals or new materials.

## 1. Introduction

Selective formation of C−C bonds using visible light (VIS) is currently at the heart of organic synthesis and holds the key to the construction of structural complexity and diversity of fine chemical, bioactive, natural, and polymeric molecules [1–7]. Such photocatalytic processes imply activated substrates that undergo facile generation of radical carbon atoms either proximal to heteroatom substituents (carbonyls, imines/enamines, malonates, etc.) or to aryl moieties [8–12], whereas the utilization of non-activated substrates has received much less attention [13–15]; their activation using VIS is currently a significantly more challenging task but would provide more effective and safer alternatives to traditional dehalogenation protocols [16,17]. In general, the energy of a visible photon edges the scope of photocatalytic bond activations [18–20], delivering insufficient energy for stronger bonds splitting such as those found in aryl(Ar)-halides [21–25]. Thus, new procedures capable of overcoming this issue would be useful to deal with this limitation.

Photon upconversion (UC) based on triplet-triplet annihilation (TTA) is one of the most attractive wavelength conversion technologies. Its interest has been intensified in the last decade due to the employment of low intensity and non-coherent light [26]. This synchronized biphotonic process transforms VIS-to-UV light which includes a bimolecular system and the association of multistep photochemical events

(Scheme S1 in the Supporting information). A variety of organic dyes and metal complexes showing TTA-UC can be found in the literature [27]. This methodology has been successfully applied in diverse scientific areas such as displays [28], bioimaging [29], phototherapy [30] or integrated TTA-UC solar cells [31], constituting nowadays a highly active area of research.

Among protocols using UVA light source[32], some recent examples have revealed that two-photon processes are suitable techniques for the activation of aryl halides (Br, Cl) using VIS [33–38]. In particular, the photogeneration of radical anions of these aryl halides leading to the reduced species has been elegantly demonstrated by the observation of a delayed fluorescence (higher energy) afforded by TTA (lower energy) [33,34]. In this context, the development of TTA-UC technology for addressing critical bond activations (e.g. hitherto unreactive aryl halides) by single electron transfer (SET) for organic synthesis may be advantageous in terms of mild reaction conditions (lower-energy VIS, room temperature and ambient pressure), metal-free photocatalyst systems [39–43] and no additives (sacrificial donors/acceptors) in the medium. With all this in mind, we report herein, as a proof of concept, a new approach into the widely studied C−C forming bond reaction by using TTA-UC technology (Fig. 1A). As far as we know, the feasibility of these cascade processes (visible light + TTA-UC + SET + Activation + Radical intermediate + C−C Coupling) to be applied in synthetic reactions such as C−C forming bonds remains still unexplored
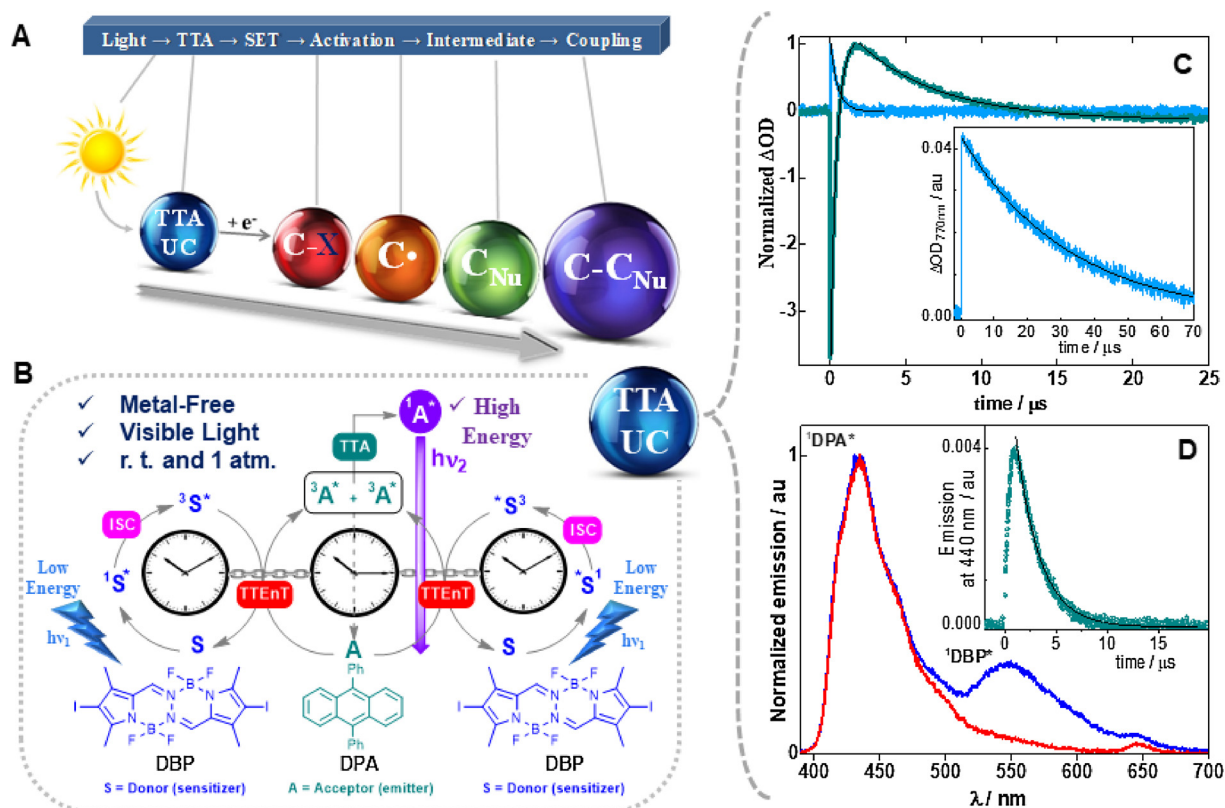
**Fig. 1. A:** Conceptual scheme: Cascade processes involving TTA-UC, single ET and reductive activation of hitherto unreactive aryl halide for C−C coupling reaction with a nucleophile-C. **B:** Schematic illustration of the photochemical events associated to the TTA-UC technology; conversion of low energy into high energy ($h\nu_1 = 2.5$ eV → $h\nu_2 = 3.1$ eV). ISC = intersystem crossing, TTEnT = triplet-triplet energy transfer, TTA = triplet-triplet annihilation. Spectroscopic evidences for the synchronized biphotonic process of **DBP**/**DPA** couple. **C:** Decay kinetics monitored at 770 nm (blue) and 430 nm (green) after 485 nm LFP of **DBP** (0.05 mM) in $N_2$/DMF solution in the presence of **DPA** (1 mM). Inset: decay kinetic monitored at 770 nm (black) after 485 nm LFP of **DBP** (0.05 mM) in $N_2$/DMF solution. **D:** Emission spectra ($\lambda_{exc} = 485$ nm) of a mixture of **DBP** (0.05 mM) and **DPA** (1 mM) in $N_2$/DMF recorded at 14 ns (blue) and 50 ns (red) after the laser pulse. Inset: Kinetic decay of the delayed ${}^1$**DPA*** at 440 nm. The black lines indicate the goodness of the lifetime measurement fitting. (For interpretation of the references to colour in this figure legend, the reader is referred to the web version of this article.)

and deserves further investigation. To test this concept, 4-bromoacetophenone (**1**) and *N*-methyl pyrrole (**2**) were chosen as reaction partners using diiodoBOPHY-like derivative (**DBP**) and 9,10-diphenylanthracene (**DPA**) as the metal-free TTA-UC system (Fig. 1B).

## 2. Main methods

### 2.1. General procedure for the C−C coupling photoreactions

In a quartz cuvette (4 mL) with a magnetic stirring bar, an ACN (2.250 mL) + DMF (0.750 mL) solution of aryl halide (30 μmol, 0.01 M, 1.0 equiv.), *N*-methyl pyrrole **2** (213 μL, 24 mmol, 0.8 M, 80 equiv.), **DBP** (100 μg, 0.3 μmol, 0.0001 M, 0.01 equiv.), **DPA** (1 mg, 3 μmol, 0.001 M, 0.1 equiv.) and 1-dodecanenitrile (6.5 μL, 0.01 M, 1 equiv.) was prepared. The cuvette was sealed with a septum and placed in a water cooling holder in order to keep a constant temperature around 20 °C (Fig. S8 in the Supporting information). The mixture was first purged with a nitrogen gas flux for 10 min, maintaining subsequently nitrogen atmosphere during the photolysis. Then, 2 h irradiation of the reaction was performed with an external diode laser pointer ($\lambda_{exc} = 445$ nm ± 10) through one face of the cuvette. The reaction progress was monitored by GC analysis. For isolation purposes, water (10 mL) was added and the aqueous phase was extracted with ethyl acetate (3 × 10 mL). The combined organic phases were washed with brine (10 mL), dried over magnesium sulfate, filtered from the drying agent and concentrated in vacuum. The crude product was purified via column chromatography on a silica gel column using a pentane/ethyl acetate mixture as the mobile phase.

### 2.2. Laser flash photolysis

Measurements were carried out with a LP980 from Edinburgh Instruments. The pump source is an optical parametric oscillator (OPO) provided with an UV extension NT242 pumped by the third Harmonic of a Nd:YAG laser model NT342A-10 from EKSPLA with typical pulse duration of 5 ns. The wavelength can be set from 210 nm to about 2600 nm, with a pulse width of about 5 nm using an OPO mod. The repetition rate was 10 Hz. The white probe light is generated by a pulsed xenon flash lamp (150 W) and passes the sample orthogonal to the pump beam. The duration of the probe pulse is 250 μs. This probe pulse is longer than the recorded time window of a measurement. A monochromator (TMS302-A, grating 150 lines/mm) disperses the probe light after it passed the sample. The probe light is then passed on to a PMT detector (Hamamatsu Photonics) to obtain the temporal resolved picture. The time resolution in each window is about 10% of the temporal window width. All components are controlled by the software L900 provided by Edinburgh.

## 3. Results and discussion

### 3.1. Suitability of the TTA-UC system

The design and synthesis of bis(difluoroboron)-1,2-bis((1H-pyrrol-2-yl)-methylene)hydrazines (BOPHYs) have been very recently established [44] and the number of reports with real applications has increased over the last two years [45–49]. Encouraged by this progressive evolution, we checked out the possibility of using a metal-free TTA-UC

system which included **DBP** as donor partner for the C−C coupling reaction (see synthesis details in the Supporting information). The presence of heavy atoms on the **DBP** core dropped heavily the fluorescence quantum yield ($\phi_F = 0.17$) [46], thus favoring the intersystem crossing to the triplets. In fact, **DBP** was used as photosensitizer for TTA-UC using **DPA** as emitter [45]; however this **DBP/DPA** system had not been applied for synthetic purposes. Furthermore, according to the absorption spectra (Fig. S1 in the Supporting information), photolysis in the blue region (450–490 nm) allowed exclusive excitation of **DBP** in the **DBP/DPA** couple that made it an appropriate choice for this work.

We started our investigations exciting selectively ($\lambda_{exc} = 485$ nm) a solution of **DBP** in deaerated *N,N*-dimethylformamide (DMF) by laser flash photolysis (LFP) in the µs domain. The T−T absorption band of **DBP** ($^3$**DBP**\*) was observed at 770 nm (Fig. S3 in the Supporting information) in agreement with literature data [45]. In our conditions, the triplet lifetime ($\tau_T$) of **DBP** was determined as 32 µs that fitted perfectly to a mono-exponential curve (inset in Fig. 1C).

In the presence of **DPA**, the $^3$**DBP**\* decay ($\tau_T = 0.4$ µs) was concomitant with the generation of the **DPA** triplet, $^3$**DPA**\* ($\tau_{growth} = 0.4$ µs), with a bimolecular quenching constant larger than $10^9$ M$^{-1}$ s$^{-1}$ indicating that the triplet-triplet energy transfer (TTEnT) was in fact very efficient (Fig. 1C). From a mono-exponential fit of the $^3$**DPA**\* kinetic decay (Fig. 1C), its lifetime was estimated as $\approx 5$ µs.
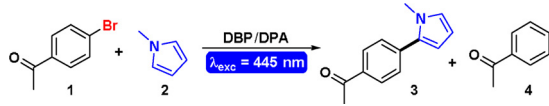
To observe the resultant formation of the **DPA** delayed fluorescence ($^1$**DPA**\*) in our conditions, a deaerated DMF solution of a mixture of **DBP/DPA** was submitted to LFP with an excitation of 485 nm. Thus, the upconverted $^1$**DPA**\* was detected displaying an emission band with maximum wavelength at 440 nm (Fig. 1D) with a singlet excited state energy of 71.5 kcal mol$^{-1}$ in DMF [34]. The **DBP** emission between $\lambda = 500–600$ nm was also observed with the incident laser pulse (Fig. 1D). Gratifyingly, the lifetime of the upconverted $^1$**DPA**\* was calculated from a mono-exponential fit of the temporal profile at 440 nm which was found to be 2.3 µs (inset in Fig. 1D). By definition [50], a P-type delayed fluorescence relies on the TTA event where two triplets (i.e., $^3$**DPA**\* + $^3$**DPA**\*) collide to populate the delayed emission (i.e. $^1$**DPA**\*). Consequently, the $^1$**DPA**\* lifetime must be approximately half that of its precursor ($^3$**DPA**\*) to ensure that the overall process is biphotonic. Taking into account these data, we clearly proved that the couple **DBP/DPA** fulfilled all of the abovementioned criteria. Furthermore, density functional theory computational studies were performed for rationalization of the TTA-UC pathways and their involved electronic configurations and transitions (Scheme S2 in the Supporting information).

### 3.2. Coupling reaction catalyzed by TTA-UC system

Once **DBP/DPA** was established as suitable TTA partners generating the high energetic $^1$**DPA**\* from lower energy light (VIS), the next step was to investigate its application to a C−C forming bond reaction. As stated above, we set out a model system which involved a non-activated aryl bromide **1** and a trapping agent such as **2** (this compound possesses high reaction rates in the adjunction of radicals) [35,38]. In addition, photolysis of a mixture of **1** and **2** in the presence of **DBP/DPA** as photocatalytic system was performed with a commercially available blue laser pointer ($\lambda_{exc} = 445$ nm ± 10, 2 W) that facilitated the management of the optimal conditions instead of using a pulsed laser from LFP technique [33,34].

In a first stage, steady-state blue light irradiation of a $N_2$/DMF mixture of **1** and **2** in the presence of catalytic amounts of **DBP/DPA** through quartz was carried out. Desired coupled product (**3**) together with the photoreduced byproduct (**4**) were formed with moderate starting material conversion and low yield (Table 1, entry 1). Although **4** was clearly the major photoproduct (DMF is a very good H-donor) [51], a reasonable amount of **3** was obtained, confirming the feasibility of the method. Control experiments were performed without **DPA** or without **DBP** (Table 1, entries 2 and 3) giving negative outcomes.

**Table 1**
Photocatalytic C−C coupling between **1** and **2** by **DBP/DPA** as TTA system.[a]



| Entry | Solvent | Conv/%[b] | 3/4[b] | Yield of 3/%[b] |
|---|---|---|---|---|
| 1 | DMF | 62[c] | 31/69 | 16 |
| 2[d] | DMF | 0 | 0/0 | – |
| 3[e] | DMF | 0 | 0/0 | – |
| 4 | ACN | 49[f] | 100/0 | 30 |
| 5 | ACN/DMF 2/1 v/v | 67 | 62/38 | 41 |
| 6 | ACN/DMF 3/1 v/v | 72 | 75/25 | 54 |
| 7[g] | ACN/DMF 3/1 v/v | 74 | 77/23 | 54 |
| **8**[h] | **ACN/DMF 3/1 v/v** | **70** | **85/15** | **60**[i] |
| 9[j] | ACN/DMF 3/1 v/v | 72 | 80/20 | 57 |
| 10[k] | ACN/DMF 3/1 v/v | 62 | 53/47 | 32 |
| 11[h] | DMA | 100 | 40/60 | 40 |
| 12 | ACN/DMA 3/1 v/v | 92 | 78/22 | 71[l] |

[a] Conditions: [**1**] = 0.01 M, [**2**] = 0.5 M, [**DBP**] = 0.1 mM, [**DPA**] = 1 mM in 3 ml of bubbled ($N_2$) solvent at 20 °C; 2 h of irradiation time with a blue laser pointer ($\lambda_{exc} = 445 \pm 10$ nm, 2 W).

[b] Conversion (conv), product distribution and yield of product **3** ([conv x selectivity of **3**%]/mass balance) were calculated from quantitative GC analysis *vs.* internal 1-dodecanenitrile. Mass balances were 100% in all cases unless otherwise indicated.

[c] 85% mass balance.

[d] Without **DPA**.

[e] Without **DBP**.

[f] 63% mass balance.

[g] 4 h of irradiation time.

[h] [**2**] = 0.8 M.

[i] Isolated yield 41%.

[j] [**2**] = 0.6 M.

[k] [**2**] = 0.25 M.

[l] Isolated yield 38%.

Employment of acetonitrile (ACN) drastically shifted the **3/4** ratio to the C−C forming bond reaction (Table 1, entry 4); however, conversion was found to be poor under the same conditions.

Aiming for the best compromise between conversion product distribution and yield of **3**, mixtures of ACN/DMF as solvent were used (Table 1, entries 5 and 6). Interestingly, a high conversion together with notable 75% selectivity to **3** and good yield were obtained when the ACN/DMF ratio was 3:1 v/v after only 2 h of irradiation time (Table 1, entry 6). Longer irradiation times did improve very slightly the result (Table 1, entry 7) whereas the presence of different amounts of **2** clearly gave changes on the product distribution (Table 1, entries 8–10); as expected, the higher equivalents of **2** the better yields of **3**. With the occurrence of decreasing the production of by-product **4**, we employed *N,N*-dimethylacetamide (DMA) as solvent (N−C(O)CH$_3$ group appears to be less acid than N−CHO group). Although conversion of **1** improved (Table 1, entries 11 and 12), similar selectivity and amounts of isolated coupling product were obtained.

### 3.3. Mechanism

To evaluate the nature of the excited state from the TTA-UC system involved in the SET process, quenching experiments were carried out by means of LFP under reaction conditions (Fig. S4 in the Supporting information). Hence, delayed fluorescence intensity of **DPA** gradually decreased upon addition of increasing amounts of **1** (normalized spectra on **DBP** emission regarding control experiment, Table 1 entry 2). Fig. 2A shows the Stern–Volmer correlation [52] (equations S1 and S2 in the Supporting information) where $K_{SV}$ was obtained as 12.8 M$^{-1}$. Considering this value and the **DPA** singlet lifetime ($\tau_F = 6.5$ ns in
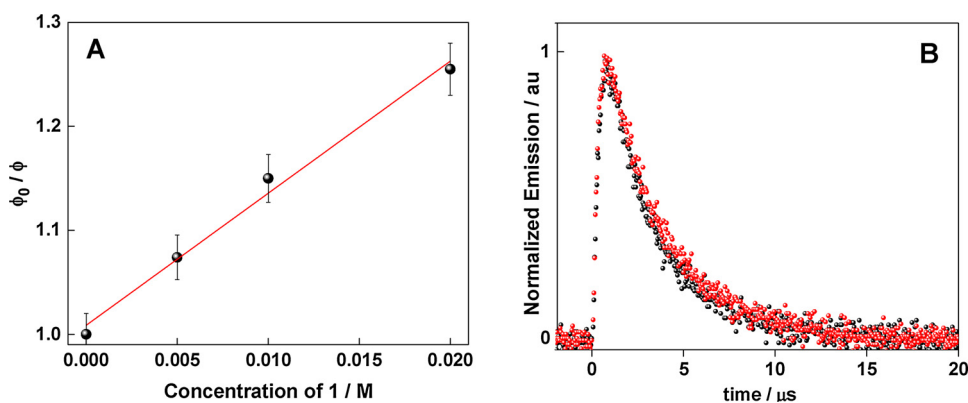
Fig. 2. Activation of target compound 1 by delayed $^1$DPA*. A: Stern-Volmer plot to obtain $k_q$ (S$_1$); experimental errors were lower than 2% of the obtained values. B: Kinetic decays of the delayed $^1$DPA* at 440 nm without 1 (black) and with 5 mM of 1 (red). (For interpretation of the references to colour in this figure legend, the reader is referred to the web version of this article.)
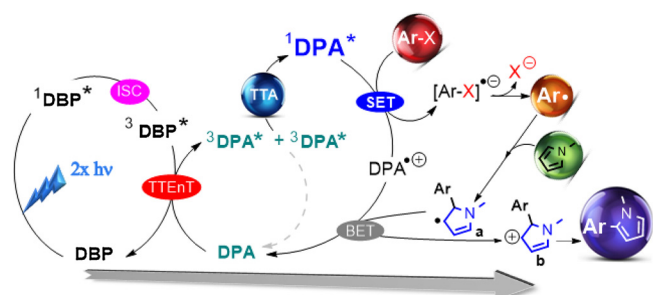


Fig. 3. Proposed photocatalytic mechanism of the C−C coupling reaction between aryl halides and N-methyl pyrrole. Cascade processes involving: ISC (intersystem crossing), TTEnT (triplet-triplet energy transfer), TTA (triplet-triplet annihilation), SET (single electron transfer), C−C bond formation and BET (back electron transfer).
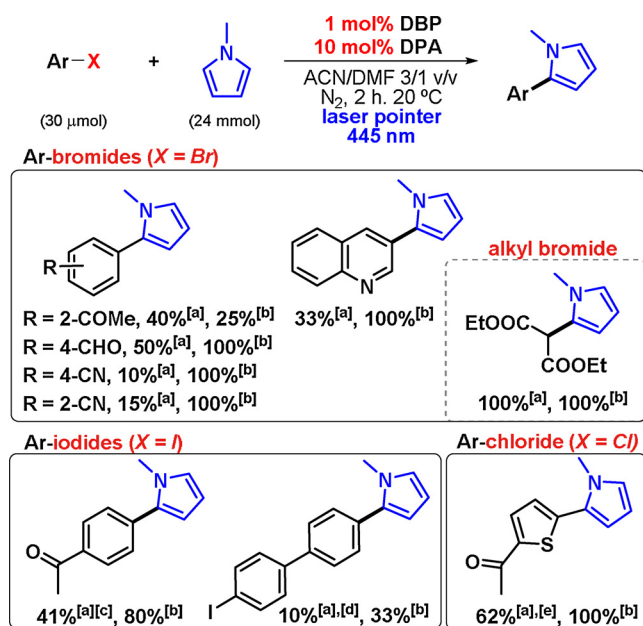


Fig. 4. Other examples of C−C coupling photoreaction using DBP/DPA as photocatalysts. Reaction conditions: aryl bromide ($10^{-2}$ M), N-methyl pyrrole (0.8 M), DBP ($10^{-4}$ M) and DPA ($10^{-3}$ M), 3 ml of ACN/DMF 3/1 v/v using a blue laser pointer (445 nm ± 10) under nitrogen atmosphere during 2 h. [a]conversion; [b]selectivity; [c]from 4-iodoacetophenone; [d]from 4,4′-diiodo-biphenyl [0.007 M], ACN/DMF 1/1 v/v, 67% selectivity of 4-iodo-1,1′-biphenyl; [e]from 2-acetyl-5-chlorothiophene.

ACN/DMF 3/1 v/v) that was experimentally obtained (Fig. S5 in the Supporting information), the fluorescence quenching rate constant, $k_q$(S$_1$), was found to be $1.9 \times 10^9$ M$^{-1}$ s$^{-1}$. From these data, 1

quenches the delayed $^1$DPA* at a nearly diffusion controlled rate.

Deactivation of $^1$DPA* under preparative irradiation conditions ([1] = 0.01 M) (equation S3 in the Supporting information) relies on the relative contribution of the different pathways which includes fluorescence, fluorescence quenching and intersystem crossing. The fluorescence ($k_F$) and intersystem crossing ($k_{ISC}$) rate constants were $k_F = 1.1 \times 10^8$ s$^{-1}$ and $k_{ISC} = 0.4 \times 10^8$ s$^{-1}$, respectively (equations S4 and S5 in the Supporting information), taking into account the quantum yields of fluorescence ($\phi_F = 0.73$, see Figs. S2 and S6 in the Supporting information) and intersystem crossing ($\phi_{ISC} = 0.27$) [53,54], respectively. Under these conditions, quenching of the delayed $^1$DPA* by 1 contributed 11% to the overall singlet deactivation with a significant residual fluorescence (65%) and some amount of the excited molecules (24%) intersystem crossing to the triplet state. Actually, observation of fluorescence quenching would not discard that activation of 1 could take place from the $^3$DPA*. Spectroscopic measurements were carried out to establish whether $^3$DPA* may or may not be correlated with the C−C coupling catalytic reaction. Thus, addition of 1 to the TTA system (0.1 mM DBP, 1 mM DPA in ACN/DMF 3/1 v/v, N$_2$, $\lambda_{exc} = 485$ nm) did not affect the temporal profile of the delayed $^1$DPA* at 440 nm (Fig. 2B). Assuming $^3$DPA* quenching by 1, there would have been a direct effect in the lifetime of the delayed $^1$DPA*. In other words, sensitized $^3$DPA* is the direct precursor of the delayed $^1$DPA* and any external factor that may affect it should have a posterior consequence. These findings therefore allowed us to conclude that activation of 1 by SET occurred from the delayed $^1$DPA*. Furthermore, ET thermodynamics strongly supported this analysis. Application of the Weller equation [55] (equation S6 in the Supporting information) was used for estimating the free energy changes ($\Delta G_{ET}$ in kcal mol$^{-1}$) associated with ET processes. The oxidation potential ($E°_{(DPA\cdot^+/DPA)}$) of DPA as well as its singlet and triplet energy $E*(S_1$ or $T_1)$ were previously reported [34,56]. Their corresponding values are 1.25 V vs. SCE, 71.5 and 41.5 kcal mol$^{-1}$, respectively. Taking into account the reduction potential of 1 ($-1.81$ V vs. SCE) [34], the $\Delta G_{ET}$ (S$_1$) and $\Delta G_{ET}$ (T$_1$) values were estimated as $-0.9$ kcal mol$^{-1}$ and $+29.5$ kcal mol$^{-1}$, respectively. Therefore, activation of 1 by delayed $^1$DPA* would be an exergonic process, whereas the mechanism from $^3$DPA* is thermodynamically prohibited.

The obtained results can be rationalized as depicted in Fig. 3. The $^3$DBP* is generated after selective excitation to DBP plus an efficient ISC. Re-establishment of DBP takes place in the presence of DPA by fast TTEnT process giving rise to the $^3$DPA* that is capable of colliding with other $^3$DPA*. This deactivating phenomenon, named TTA, affords the formation of a delayed fluorescence $^1$DPA* possessing high-energy characteristic, sufficient to activate electrophilic substrates such as 1 by SET. Once the radical ion pairs are formed, the unstable radical anion Ar-X·$^-$ undergoes fast irreversible fragmentation to give anion X$^-$ and the aryl radical Ar· which, suitably, can be trapped by a nucleophile agent such as 2. Oxidation of the resultant radical intermediate a occurs by an exergonic BET based on DFT calculations, (Fig. S7 in the
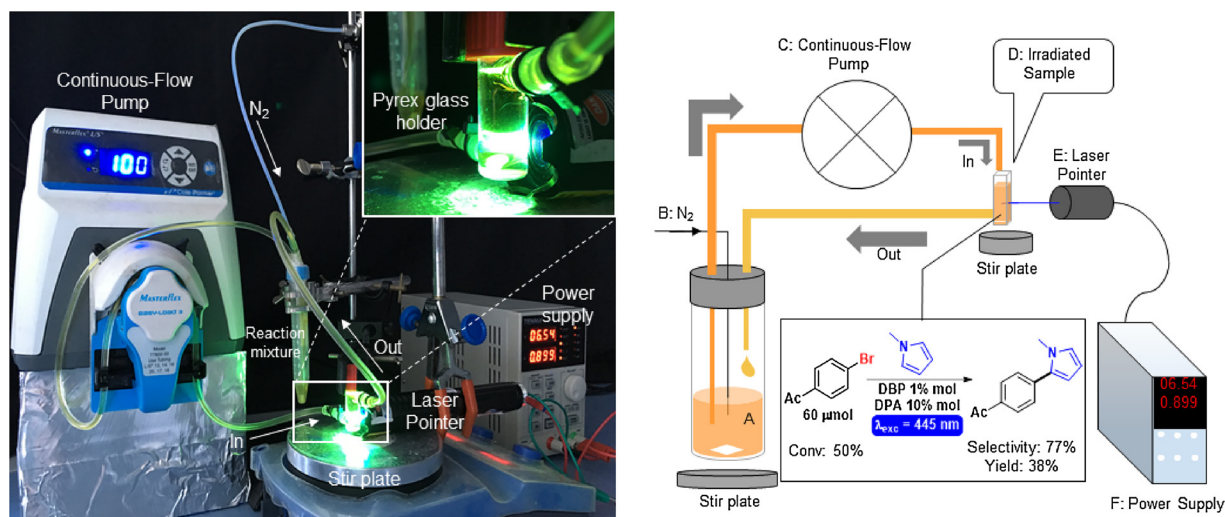
**Fig. 5.** Set-up of the continuous-flow photochemistry system. Photographs and schematic representation of the home-made continuous-flow photoreactor that demonstrates the technology transfer of C−C coupling reaction by means of TTA-UC.

Supporting information), restoring **DPA** (Fig. S9 in the Supporting information) and leading to cation intermediate **b** and afterwards to the desired couple product.

### 3.4. Scope

A few more examples of the C−C coupling catalytic reaction by **DBP**/**DPA** TTA-UC system, which strongly support the proof of concept, are shown in Fig. 4. A range of substituted aryl halides gave the corresponding coupling products where their diverse reactivity would be associated with the thermodynamic and kinetic data determined by DFT methodology at the B3LYP/6-311 + +G(d,p) level (Table S1 in the Supporting information). Regarding the activation barriers, for instance ET vs BET, low reactivity can be a direct consequence of reversibility of the electron transfer and subsequent mesolysis. Alkylation of **2** was also applied under same conditions.

### 3.5. Continuous-flow device

An up-to-date overview on photochemical transformations in continuous-flow reactors has been recently reported [57]. As a matter of fact, it would be of great interest to explore the applicability of this proof of concept with continuous-flow conditions that currently no precedents can be found in literature. Thus, the C−C coupling reaction between **1** and **2** in the presence of the TTA system (**DBP** + **DPA**) with *scaling-up* optimal conditions was actually observed under flow settings (Fig. 5). The deaerated solution phase (A) was delivered to a Pyrex glass holder (D) by a MasterFlex® continuous-flow pump (C) at 100 rpm through a Tygon® tubing (ID 1.6 mm). Constant stirring at D was achieved in order to facilitate the solution flow and minimize the possible retention time in the irradiation region. At this point, the reaction mixture was photolyzed by a blue laser pointer ($\lambda_{exc}$ = 445 nm ± 10). The final exiting stream was collected again in A to evolve continuously the photoreaction. To our delight, selectivity and isolated yield of coupled photoproduct **3** was found to be very promising and we expect that advantages of photochemical syntheses observed on a small scale will be able to be exploited on a larger scale and consequently to be implemented in the industry.

### 4. Conclusions

In conclusion, we have proven the feasibility of photon upconversion technology based on triplet-triplet annihilation to be successfully applied to organic synthesis such as heteroarene functionalization by a C−C coupling reaction. The approach follows an unprecedented cascade of processes that involves both photophysical (ISC, TTET, TTA) and photochemical (SET, radical trapping, C−C forming bond) events as crucial steps. Combination of spectroscopic data, product analysis and theoretical calculations support the described mechanistic scenario (Fig. 4). It is worth highlighting the advantages of this catalytic protocol, which includes very mild reaction conditions (visible light, room temperature and ambient pressure), employment of metal-free photocatalysts and no additives (sacrificial donors/acceptors) in the medium. We believe that this original methodology will make way for applications to the synthesis of fine chemical building blocks, pharmaceuticals, agrochemicals or new materials and therefore to have an immediate impact on the current state of industrial manufacture.

### Competing financial interests

The authors declare no competing financial interests.

### Acknowledgements

### Appendix A. Supplementary data

Supplementary material related to this article can be found, in the online version, at doi:https://doi.org/10.1016/j.apcatb.2018.05.062.

### References

[1] D. Ravelli, S. Protti, M. Fagnoni, Carbon−carbon bond forming reactions via photogenerated intermediates, Chem. Rev. 116 (2016) 9850–9913.
[2] M. Fagnoni, D. Dondi, D. Ravelli, A. Albini, Photocatalysis for the formation of C−C bond, Chem. Rev. 107 (2007) 2725–2756.
[3] J.M.R. Narayanam, C.R.J. Stephenson, Visible light photoredox catalysis: applications in organic synthesis, Chem. Soc. Rev. 40 (2011) 102–113.

[4] D.M. Schultz, T.P. Yoon, Solar synthesis: prospects in visible light photocatalysis, Science 343 (2014) 985.

[5] C.K. Prier, D.A. Rankic, D.W.C. MacMillan, Visible light photoredox catalysis with transition metal complexes: applications in organic synthesis, Chem. Rev. 113 (2013) 5322–5363.

[6] C.R. Jamison, L.E. Overman, Fragment coupling with tertiary radicals generated by visible-light photocatalysis, Acc. Chem. Res. 49 (2016) 1578–1586.

[7] N.A. Romero, D.A. Nicewicz, Organic photoredox catalysis, Chem. Rev. 116 (2016) 10075–10166.

[8] F. Teply, Photoredox catalysis by [Ru(bpy)3]2+ to trigger transformations of organic molecules. Organic synthesis using visible-light photocatalysis and its 20th century roots, Collect. Czech. Chem. Commun. 76 (2011) 859–917.

[9] D.A. Nicewicz, D.W.C. MacMillan, Merging photoredox catalysis with organocatalysis: the direct asymmetric alkylation of aldehydes, Science 322 (2008) 77–80.

[10] K. Zeitler, Photoredox catalysis with visible light, Angew. Chem. Int. Ed. 48 (2009) 9785–9789.

[11] J.W. Beatty, C.R.J. Stephenson, Amine functionalization via oxidative photoredox catalysis: methodology development and complex molecule synthesis, Acc. Chem. Res. 48 (2015) 1474–1484.

[12] K. Nakajima, Y. Miyake, Y. Nishibayashi, Synthetic utilization of α-aminoalkyl radicals and related species in visible light photoredox catalysis, Acc. Chem. Res. 49 (2016) 1946–1956.

[13] Y. Jin, H. Fu, Visible-light photoredox decarboxylative couplings, Asian J. Org. Chem. 6 (2017) 368–385.

[14] M. Májek, A. Jacobi von Wangelin, Mechanistic perspectives on organic photoredox catalysis for aromatic substitutions, Acc. Chem. Res. 49 (2016) 2316–2327.

[15] J. Xuan, Z.-G. Zhang, W.-J. Xiao, Visible-light-induced decarboxylative functionalization of carboxylic acids and their derivatives, Angew. Chem. Int. Ed. 54 (2015) 15632–15641.

[16] P. Knochel, W. Dohle, N. Gommermann, F.F. Kneisel, F. Kopp, T. Korn, I. Sapountzis, V.A. Vu, Highly functionalized organomagnesium reagents prepared through halogen-metal exchange, Angew. Chem. Int. Ed. 42 (2003) 4302–4320.

[17] A. Krief, A.-M. Laval, Coupling of organic halides with carbonyl compounds promoted by SmI2, the Kagan reagent, Chem. Rev. 99 (1999) 745–778.

[18] T.P. Yoon, M.A. Ischay, J. Du, Visible light photocatalysis as a greener approach to photochemical synthesis, Nat. Chem. 2 (2010) 527–532.

[19] D. Ravelli, S. Protti, M. Fagnoni, A. Albini, Visible light photocatalysis: a green choice? Curr. Org. Chem. 17 (2013) 2366–2373.

[20] M. Reckenthäler, A.G. Griesbeck, Photoredox catalysis for organic syntheses, Adv. Synth. Catal. 355 (2013) 2727–2744.

[21] E. Abitelli, S. Protti, M. Fagnoni, A. Albini, Probing for a leaving group effect on the generation and reactivity of phenyl cations, J. Org. Chem. 77 (2012) 3501–3507 Other mechanisms operate in such bond activations: by UV irradiation:.

[22] L. Shi, W. Xia, Photoredox functionalization of C−H bonds adjacent to a nitrogen atom, Chem. Soc. Rev. 41 (2012) 7687–7697 Via N-oxidation:.

[23] S. Protti, M. Fagnoni, D. Ravelli, Photocatalytic C−H activation by hydrogen-atom transfer in synthesis, Chem. Cat. Chem. 7 (2015) 1516–1523 Via H atom transfer:.

[24] C.K. Prier, D.W.C. MacMillan, Amine α-heteroarylation via photoredox catalysis: a homolytic aromatic substitution pathway, Chem. Sci. 5 (2014) 4173–4178 Via amine oxidation:.

[25] D.C. Fabry, J. Zoller, S. Raja, M. Rueping, Combining rhodium and photoredox catalysis for C−H functionalizations of arenes: oxidative heck reactions with visible light, Angew. Chem. Int. Ed. 53 (2014) 10228–10231 Metal co-catalysis:.

[26] C. Ye, L. Zhou, X. Wang, Z. Liang, Photon upconversion: from two-photon absorption (TPA) to triplet-triplet annihilation (TTA), Phys. Chem. Chem. Phys. 18 (2016) 10818–10835.

[27] T.N. Singh-Rachford, F.N. Castellano, Photon upconversion based on sensitized triplet-triplet annihilation, Coord. Chem. Rev. 254 (2010) 2560–2573.

[28] T. Miteva, V. Yakutkin, G. Nelles, S. Baluschev, Annihilation assisted upconversion: all-organic, flexible and transparent multicolour display, New J. Phys. 10 (2008) 103002.

[29] Q. Dou, L. Jiang, D. Kai, C. Owh, X.J. Loh, Bioimaging and biodetection assisted with TTA-UC materials, Drug Discov. Today 22 (2017) 1400–1411.

[30] M.E. Lim, Y.-l. Lee, Y. Zhang, J.J.H. Chu, Photodynamic inactivation of viruses using upconversion nanoparticles, Biomaterials 33 (2012) 1912–1920.

[31] S.P. Hill, T. Dilbeck, E. Baduell, K. Hanson, Integrated photon upconversion solar cell via molecular self-assembled bilayers, ACS Energy Lett. 1 (2016) 3–8.

[32] E.H. Discekici, N.J. Treat, S.O. Poelma, K.M. Mattson, Z.M. Hudson, Y. Luo, C.J. Hawker, J. Read de Alaniz, A highly reducing metal-free photoredox catalyst: design and application in radical dehalogenations, Chem. Commun. 51 (2015) 11705–11708 See for example:.

[33] M. Majek, U. Faltermeier, B. Dick, R. Perez-Ruiz, A. Jacobi von Wangelin, Application of visible-to-uv photon upconversion to photoredox catalysis: the activation of aryl bromides, Chem. Eur. J. 21 (2015) 15496–15501.

[34] M. Haering, R. Perez-Ruiz, A. Jacobi von Wangelin, D. Diaz Diaz, Intragel photoreduction of aryl halides by green-to-blue upconversion under aerobic conditions,

[35] I. Ghosh, T. Ghosh, J.I. Bardagi, B. König, Reduction of aryl halides by consecutive visible light-induced electron transfer processes, Science 346 (2014) 725–728.

[36] L. Marzo, I. Ghosh, F. Esteban, B. König, Metal-free photocatalyzed cross coupling of bromoheteroarenes with pyrroles, ACS Catal. 6 (2016) 6780–6784.

[37] I. Ghosh, B. König, Chromoselective photocatalysis: controlled bond activation through light-color regulation of redox potentials, Angew. Chem. Int. Ed. 55 (2016) 7676–7679.

[38] M. Neumeier, D. Sampedro, M. Majek, V. de la Peña O'Shea, A. Jacobi von Wangelin, R. Perez-Ruiz, Dichromatic photocatalytic substitutions of aryl halides by a small organic dye, Chem. Eur. J. 24 (2018) 105–108.

[39] A. Savateev, B. Kurpil, A. Mischenko, G. Zhang, M. Antonietti, "Waiting" carbon nitride radical anion: charge storage material and key intermediate in direct C−H thiolation of methylarenes using elemental sulfur as "S"-source, Chem. Sci. 9 (2018) 3584–3591.

[40] B. Kurpil, K. Otte, M. Antonietti, A. Savateev, Photooxidation of N-acylhydrazones to 1,3,4-oxadiazoles catalyzed by heterogeneous visible-light-active carbon nitrid semiconductor, . Appl. Catal. B 228 (2018) 97–102.

[41] L. Li, D. Cruz, O. Savatieiev, G. Zhang, M. Antonietti, Y. Zhao, Photocatalytic cyanation of carbon nitride scaffolds: tuning band structure and enhancing the performance in green light driven C−S bond formation, Appl. Catal. B 229 (2018) 249–253.

[42] B. Kurpil, B. Kumru, T. Heil, M. Antonietti, A. Savateev, Carbon nitride creates thioamides in high yields by the photocatalytic Kindler reaction, Green Chem. 20 (2018) 838–842.

[43] A. Savateev, D. Dontsova, B. Kurpil, M. Antonietti, Highly crystalline poly(heptazine imides) by mechanochemical synthesis for photooxidation of various organic substrates using an intriguing electron acceptor-elemental sulfur, J. Catal. 350 (2017) 203–211.

[44] I.-S. Tamgho, A. Hashemimasab, J.T. Engle, V.N. Nemykin, C.J. Ziegler, A new highly fluorescent and symmetric pyrrole-BF2 chromophore: BOPHY, J. Am. Chem. Soc. 136 (2014) 5623–5626.

[45] C. Zhang, J. Zhao, Triplet excited state of diiodoBOPHY derivatives: preparation, study of photophysical properties and application in triplet-triplet annihilation upconversion, J. Mater. Chem. C 4 (2016) 1623–1632.

[46] Q. Huaulme, A. Mirloup, P. Retailleau, R. Ziessel, Synthesis of highly functionalized bophy chromophores displaying large stokes shifts, Org. Lett. 17 (2015) 2246–2249.

[47] A. Mirloup, Q. Huaulme, N. Leclerc, P. Lévêque, T. Heiser, P. Retailleau, R. Ziessel, Thienyl-BOPHY dyes as promising templates for bulk heterojunction solar cells, Chem. Commun. 51 (2015) 14742–14745.

[48] Y. Li, H. Zhou, S. Yin, H. Jiang, N. Niu, H. Huang, S.A. Shahzad, C. Yu, A BOPHY probe for the fluorescence turn-on detection of Cu2+, Sens. Actuators B 235 (2016) 33–38.

[49] X.-D. Jiang, Y. Su, S. Yue, C. Li, H. Yu, H. Zhang, C.-L. Sun, L.-J. Xiao, Synthesis of mono-(p-dimethylamino)styryl-containing BOPHY dye for a turn-on pH sensor, RSC Adv. 5 (2015) 16735–16739.

[50] A.D. McNaught, A. Wilkinson, IUPAC Compendium of Chemical Terminology, RSC, Cambridge, (1997), http://dx.doi.org/10.1351/goldbook.D01579 (Accessed 30th January 2018).

[51] M. Majek, F. Filace, A. Jacobi von Wangelin, Visible light driven hydro-/deuterodefunctionalization of anilines, Chem. Eur. J. 21 (2015) 4518–4522.

[52] A.D. McNaught, A. Wilkinson, IUPAC Compendium of Chemical Terminology, RSC, Cambridge, (1997), http://dx.doi.org/10.1351/goldbook.S06004 (Accessed 30th January 2018).

[53] In principle, non-radiative quantum yield ($\phi_{nr} = 1 - \phi_F$) relies on both vibrational relaxation and intersystem crossing. According to literature data (ref. 54), $\phi_{ISC}$ of DPA has been found to be ca. 0.02–0.04 in non-polar solvents such as cyclohexane or benzene. We believe that $\phi_{ISC}$ value in acetonitrile/N,N-dimethylformamide mixture may not differ too much with respect to these data. Although we assume that $\phi_{ISC}$ is 0.27, it is probably that triplet production of DPA is lower, enhancing actually the fluorescence quenching pathway.

[54] K. Suzuki, A. Kobayashi, S. Kaneko, K. Takehira, T. Yoshihara, H. Ishida, Y. Shiina, S. Oishic, S. Tobita, Reevaluation of absolute luminescence quantum yields of standard solutions using a spectrometer with an integrating sphere and a back-thinned CCD detector, Phys. Chem. Chem. Phys. 11 (2009) 9850–9860.

[55] A. Weller, Photoinduced electron transfer in solution: exciplex and radical ion pair formation free enthalpies and their solvent dependence, Z. Phys. Chem. 133 (1982) 93–98.

[56] F.E. Beideman, D.M. Hercules, Electrogenerated chemiluminescence from 9,10-diphenylanthracene cations reacting with radical anions, J. Phys. Chem. 83 (1979) 2203–2209.

[57] D. Cambié, C. Bottecchia, N.J.W. Straathof, V. Hessel, T. Noël, Applications of continuous-flow photochemistry in organic synthesis, material sciences, and water treatment, Chem. Rev. 116 (2016) 10276–10341.